FAR FIELD RADIATION IN SUB-PICOSECOND SYSTEMS

K.A. Remley, A. Weisshaar, S.M. Goodnick and V.K. Tripathi

Department of Electrical and Computer Engineering
Oregon State University
Corvallis, Oregon, USA 97331

Abstract—**FDTD and Monte Carlo methods are combined to simulate the terahertz radiation fields from a coplanar photoconducting structure. Two techniques are considered for modeling the far field radiation. One uses Maxwell's equations directly with an approximation made regarding the source term. As an improvement to the first technique, we propose the use of a near-to-far-field FDTD transformation with the use of equivalent surface current densities. Computational results showing the far field radiation are in agreement with published experimental results.**

INTRODUCTION

Characterization of the electromagnetic radiation arising from devices which operate in the millimeter or submillimeter range is important, particularly for devices whose dimensions approach the wavelength of operation. Analysis of this radiation is of interest in crosstalk and interference analyses, where the radiation may have a detrimental effect on system operation. The radiation may be used to advantage in other applications, such as the characterization of materials by electooptic sampling and terahertz spectroscopy [1] [2], and with submillimeter-wave and terahertz radiators [3] [4]. An accurate representation of the far field radiation is desirable in each of these cases.

The simulation tool under consideration couples a Monte Carlo particle simulator to either a Poisson solver or a Finite Difference Time Domain (FDTD) electromagnetic solver to determine the high frequency device characteristics. Potentials, particle distributions, current densities, and the near field electromagnetic fields may be determined anywhere in the computational domain. This type of tool has been used in the analysis of MESFETs and MODFETs [5] [6] as well as in simulation of photoconductive switch experiments [7]. For analysis of devices with a radiative element, the FDTD method is used in the simulator. It is not efficient or, in many cases, physically possible at present to calculate far field radiation directly using the FDTD technique because of the excessive computational burden.

In the present work we will demonstrate two alternate techniques for modeling the far field radiation. The first involves calculation of the electric field directly from the time-varying current source(s) in the device through Maxwell's equations. This technique is commonly used in the solution of this problem, however, it has the disadvantage that it is difficult to accurately incorporate the effects of the varying source material parameters. An alternate technique is proposed using the time-domain near-to-far-field transformation [10] [11]. This technique incorporates an equivalent source methodology commonly used by microwave and RF engineers for the analysis of radiation from, for example, horn antennas [12]. Equivalent surface currents are found from the tangential electric and magnetic fields on a virtual surface (or aperture) in the vicinity of the actual source of radiation. These equivalent surface currents are used as new sources of radiation in a homogeneous problem space. The two computational techniques for determining the far field are discussed in the following.

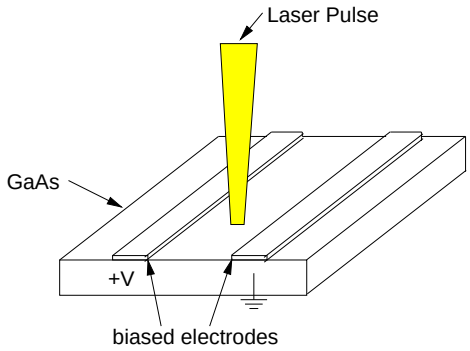

Fig. 1. Typical structure for an electrooptic sampling experiment.

THEORY

To illustrate the computational techniques, an electrooptic sampling experiment is simulated, as shown in Figure (1). In this type of experiment, a laser pulse incident on a GaAs substrate creates electron-hole pairs. Biased electrodes on either side of the laser pulse cause the electrons and holes to migrate away from each other slightly, creating a dipole moment. The movement of the electrons and holes induces a time-varying current density in the GaAs substrate. Figure (2) illustrates typical electron-hole separation with time. The current pulse created in the GaAs substrate has an extremely fast rise time, from a few hundred femtoseconds to a few picoseconds. Once the excitation is removed, the biased electrodes continue to attract the electrons and holes. Recombination is minimal and, therefore, the dipole exists for a time much longer than the simulation.

0-7803-4603-6/97/$5.00 (c) IEEE

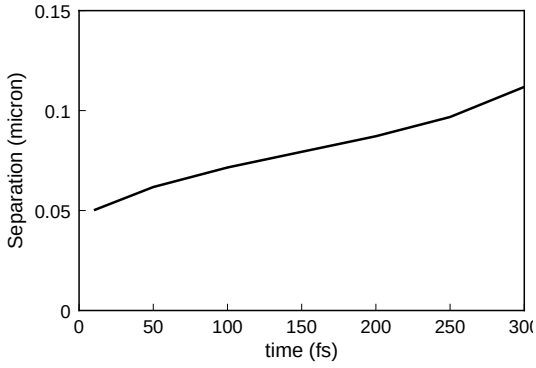

Fig. 2. Typical separation of electrons and holes with time.

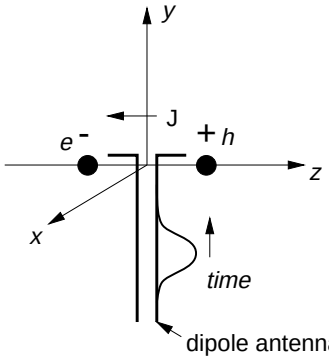

Fig. 3. Equivalent dipole representation.

The current pulse is the source of an electromagnetic radiation field which propagates away from the GaAs substrate. The radiation pulse can be extremely fast, in the GHz to low THz range [1] [13]. As shown in Figure (3), the dipole may be modeled as an antenna. The far field radiation can be calculated in the time domain from through the relation:

$$E_\theta(r,t) \approx \frac{\sin\theta}{4\pi\epsilon_0 r c^2}\frac{\partial}{\partial t}\iiint_{V'} \vec{J}_V\, dV' \qquad (1)$$

where r is the distance from the dipole to the far field observation point, J is the volume current density induced by the dipole, and θ is measured off the axis of the dipole (the z axis).

The far field model based on the current pulse calculation assumes an ideal dipole as a source and propagation in free space. The presence of the GaAs substrate will introduce some inaccuracy into the calculation. To eliminate this source of error, a near-to-far-zone field transformation is proposed. In this technique [9], equivalent electric and magnetic surface current densities are found on a virtual surface, S, which separates the inhomogeneous region. The equivalent surface current densities are found through the following relations:

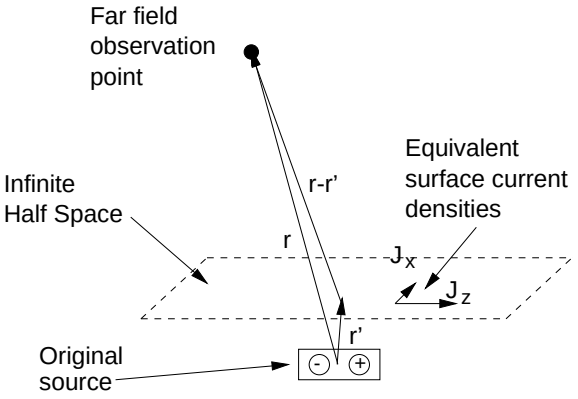

Fig. 4. Equivalent current source model.

$$J_s = \hat{n} \times \vec{H} \qquad (2)$$
$$M_s = -\hat{n} \times \vec{E} \qquad (3)$$

See Figure (4). These surface current densities are used as a new source of radiation, and the far zone electric field may be found as

$$E_\theta(\bar{r},t) \approx -\eta_0 W_\theta(\bar{r},t) - U_\phi(\bar{r},t) \qquad (4)$$
$$E_\phi(\bar{r},t) \approx -\eta_0 W_\phi(\bar{r},t) + U_\theta(\bar{r},t) \qquad (5)$$

with vector potentials $\vec{W}$ and $\vec{U}$ given as follows:

$$\vec{W}(\bar{r},t) = \frac{1}{4\pi r c}\frac{\partial}{\partial t}\left[\iint_S \vec{J}_s\left(t - \frac{r - \bar{r}'\cdot\hat{r}}{c}\right) dS'\right] \qquad (6)$$
$$\vec{U}(\bar{r},t) = \frac{1}{4\pi r c}\frac{\partial}{\partial t}\left[\iint_S \vec{M}_s\left(t - \frac{r - \bar{r}'\cdot\hat{r}}{c}\right) dS'\right] \qquad (7)$$

where $\bar{r}$ is the vector from the origin to the observation point in the far field and $\bar{r}'$ is the vector from the origin to the surface current element. The finite difference implementation is given in detail in [10] and [11] and will not be repeated here.

Computational Results

The modeling tool used in the present work combines a Monte Carlo particle simulator with an FDTD E-M solver. The computational domain is divided spatially into a grid. The Monte Carlo simulator is terminated in Mur first order absorbing boundary conditions, and the FDTD field solver is terminated in the Perfectly Matched Layer (PML) absorbing boundary conditions [8].

The computational algorithm used is as follows:

1) The potentials in the grid are initialized using a Poisson solver

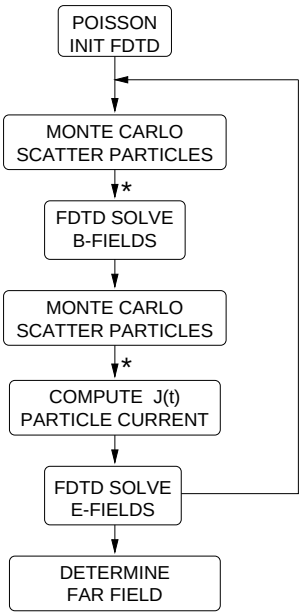

Fig. 5. Computer algorithm used in the present work.

2) Over a given period of time, particles are injected into the computational domain to simulate the incident laser pulse. The rate at which the particles are injected increases with time to a predetermined injection rate.

3) At each time step, random particle free flights are terminated in stochastically determined scattering events and FDTD field computations are alternated in a leap frog manner. Electric fields are calculated at one time step and magnetic fields are calculated at the next time step.

4) The far field profile is calculated using one of the two techniques described below.

Figure (6b) shows the simulated current pulse in the GaAs substrate for an injection rate of 1e15/cm^3 and a bias of 40 volts. The pulse was sampled and the time derivative calculated. This is shown in Figure (6b), where the thicker line is a smoothed version of the derivative. The calculated field is similar to published measurements, for example [13].

To account for the presence of an inhomogeneous substrate, including GaAs and the metal electrodes, the near-to-far field transformation was used. A decimated version of the current pulse shown in Figure (6b) was used as a z-oriented Hertzian dipole source for the FDTD simulation. The near field was calculated using FDTD along a virtual surface above the substrate. The E_z component of the near field is shown in Figure (7a) and is compared to that of an ideal dipole in Figure (7b). FDTD simulations are generally quite sensitive to transient source or field perturbations. Test sources are often designed to provide continuity of both derivative and integral in order to minimize time dispersive artifacts. It is therefore to be expected that the current pulse

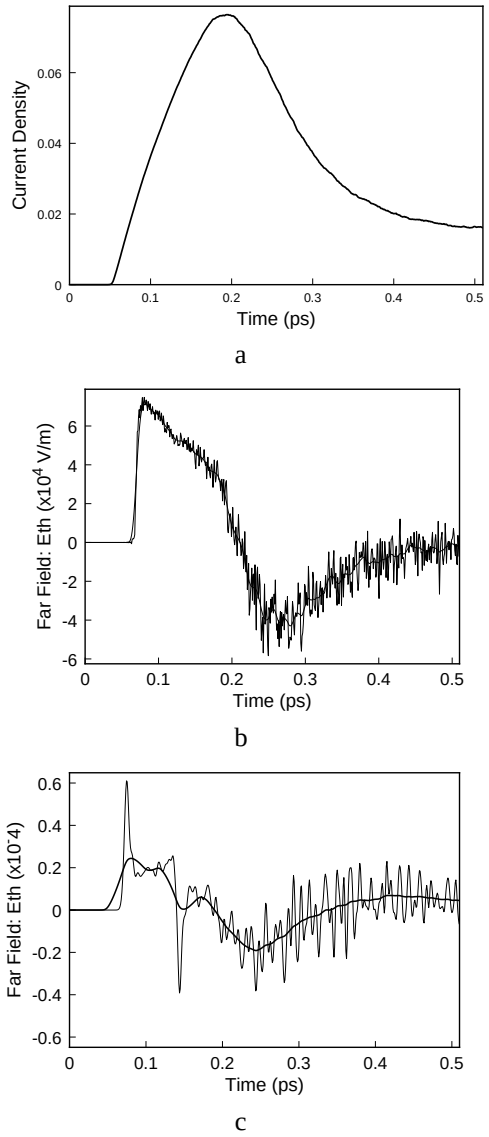

Fig. 6. (a) Current density in the GaAs substrate for an injection rate of 1e15/cm^3 and bias of 40 volts. (b) Time derviative of the current pulse shown in (a). The thicker line is a numerically smoothed version of the original. (c) Near-to-far field transformation with smoothed version superimposed.

shown in Figure (6b), when used as a source, will generate many transient effects (see Figure (6c)). However, with signal post-processing, information may be obtained from the data. For example, the delay in the arrival time of the far field caused by the presence of inhomogenous material such as the GaAs substrate may found by comparing the far field transformation results for a structure with and without the inhomogeneous material. Delays which may be difficult to analyze directly, such as those from a distributed source, may be simulated using this technique.

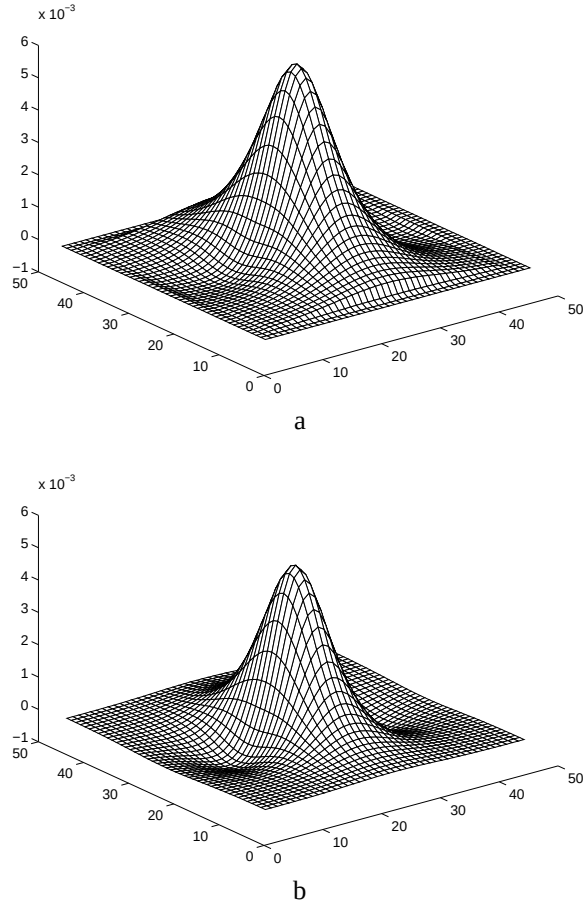

Fig. 7. (a) The E_z component of the near field radiation along a plane above and parallel to the GaAs substrate. (b) The E_z component with an ideal dipole source. Axes show number of grid points.

CONCLUSION

Two techniques for modeling the far field radiation from millimeter-wave and submillimeter-wave devices have been presented. One is based on direct calculation of the far field approximation derived from Maxwell's equations. The other formulation is based on equivalent surface current densities used as equivalent sources of radiation in a homogeneous problem space. With signal processing, the direct calculation enables a first order approximation of the radiation arising from ultrafast electronic devices. The near-to-far field transformation allows determination of the effects of an inhomogeneous problem space.

ACKNOWLEGEMENTS

This work is supported by a grant from the National Science Foundation. K. Remley is also supported under a National Science Foundation Graduate Research Fellowship.

REFERENCES

[1] J. Valdmanis and G. Mourou, "Subpicosecond electrooptic sampling: principles and applications," *IEEE J. Quantum Electron.*, vol. QE-22, pp. 69–78, Jan. 1986.

[2] B. Greene, J. Federici, D. Dykaar, A. Levi, and L. Pfeiffer, "Picosecond pump and probe spectroscopy utilizing freely propagating terahertz radiation," *Opt. Lett.*, vol. 16, pp. 48–49, Jan. 1991.

[3] P. R. Smith, D. H. Auston, and M. Nuss, "Subpicosecond photoconducting dipole antennas," *IEEE J. Quantum Electron.*, vol. 24, pp. 255–260, Feb. 1988.

[4] N. Froberg, B. Hu, X. Zhang, and D. H. Auston, "Terahertz radiation from a photoconducting antenna array," *IEEE J. Quantum Electron.*, vol. 28, pp. 2291–2301, Oct. 1992.

[5] S. Goodnick, S. Pennathur, U. Ranawake, P. Lenders, and V. Tripathi, "Parallel implementation of a Monte Carlo particle simulation coupled to Maxwell's equations," *Intl. J. of Num. Modelling*, vol. 8, pp. 205–219, 1995.

[6] S. Sohel Imtiaz, M. Llsunaidi, and S. El-Ghazaly, "Performance comparison of MODFET and MESFET using combined electromagnetic and solid-state simulator," in *International Microwave Symposium Digest*, pp. 1783–1786, San Francisco, CA, USA, 1996.

[7] S. El-Ghazaly, F. Joshi, and R. Grondin, "Electromagnetic and transport considerations in subpicosecond photoconductive switch modeling," *IEEE Trans. Microwave Theory Tech.*, vol. 38, pp. 629–637, May 1990.

[8] J. P. Berenger, "A perfectly matched layer for the absorption of electromagnetic waves", *J. Computational Physics*, vol. 114, pp. 185–200, 1994.

[9] S. A. Schelkunoff,"Some equivalence theorems of electromagnetics and their application to radiation problems," *Bell System Tech. J.*, vol. 15, pp. 92-112, 1936.

[10] K. S. Kunz and R. Luebbers, *The Finite Difference Time Domain Method for Electromagnetics*. Boca Raton: CRC Press, 1993.

[11] A. Taflove, *Computational Electrodynamics The Finite-Difference Time-Domain Method*. Boston: Artech House, 1995.

[12] C. Balanis, *Advanced Engineering Electromagnetics*. New York: Wiley, 1989.

[13] J. Son, W. Sha, T. Norris, J. Whitaker, and G. Mourou, "Transient velocity overshoot dynamics in GaAs for electric fields <200kV/cm," *Appl. Phys. Lett.*, vol. 63, pp. 923–925, Aug. 1993.